J. Mol. Biol. (1974) 87, 641–656

Electron Microscopy of the Stacked Disk Aggregate of Tobacco Mosaic Virus Protein

I. Three-dimensional Image Reconstruction

P. N. T. Unwin and A. Klug

Medical Research Council Laboratory of Molecular Biology
Hills Road, Cambridge CB2 2QH, England

(Received 22 February 1974)

The three-dimensional structure of the stacked disk aggregate of tobacco mosaic virus protein has been determined from "phase plate" electron micrographs to an effective resolution of about 12 Å. It is a long rod comprised of paired rings of protein (disks), the subunits of which have different conformations according to which ring they belong. The two subunit conformations are such that the rings come close together within a disk near the outer surface of the particle, but between disks on the inside. This property, interpreted on the basis of a polar packing of the subunits, was established from an earlier, lower resolution, study by Finch & Klug (1971). The present study shows, in addition, that the pairing is contributed mainly by axial distortions of the subunits in one of the rings, the axial distortions of the subunits in the other being largely replaced at lower radii by a tilt or twist and, at higher radii, by a slew. The subunits in the latter ring appear to have a conformation similar to that of the protein molecules in the virus.

1. Introduction

The stacked disk aggregate of tobacco mosaic virus (TMV) protein is one of several kinds of organized structures it is possible to form from TMV coat protein under varying conditions of pH and ionic strength. Its existence was first inferred nearly 20 years ago (Franklin & Commoner, 1955) from X-ray diffraction patterns of the polymerized protein isolated from infected plants, and it is now known (Finch & Klug, 1971,1974) to be a long rod built up from disks of these protein molecules so stacked that each successive one has a small rotational stagger (3/10 of $2\pi/17$ rad) with respect to the one preceding it. The disk, moreover, has been well characterized as a discrete structure made up from two coaxial rings, each of 17 protein subunits (Finch *et al.*, 1966); its biological significance, recently established by Butler & Klug (1971), is that it plays a key role in the assembly of a complete virus.

The most thorough previous investigation of the stacked disk aggregate has been by bright field electron microscopy of negatively stained specimens (Finch & Klug, 1971) in conjunction with a three-dimensional reconstruction technique (DeRosier & Klug, 1968) to analyse the images. One of the main concerns of this investigation was to establish the polarity of the subunits in each of the two layers of a disk. Although a cursory examination of the electron micrographs might suggest that the subunits in the two layers are paired so as to be related dyadically (i.e. front against

front), the analysis in fact favoured the alternative—that they are stacked in a polar manner (i.e. front against back) just as in the virus. The reasons for concluding that the stacking is polar were based on the findings of the three-dimensional analysis that the subunits in the two layers were not distorted axially by the same amount, a feature which would be consistent with a perturbed polar structure (Caspar, 1963), and also that at an outer radius the subunits slewed similarly in the same direction.

Evidence of slewing at an outer radius has also been obtained from single (or short stacks of) disks viewed end on and analysed by a rotational filtering method (Crowther & Amos, 1971). With this method, however, it is not possible to confirm that there is a similar slewing of the subunits in both layers; the features observed in the rotationally filtered images could, for instance, be accounted for by a slewing in only one of the two layers.

Recent X-ray studies of crystals of disks (Gilbert & Klug, 1974) appear to confirm the deductions made from electron micrographs that the stacking of the subunits in the two layers is polar. It is likely, however, that there are some structural differences between the disks in the two polymorphic forms, brought about by their different packing arrangements and the fact that in the rod-shaped polymer some of the protein is proteolytically cleaved (Durham, 1972).

In the present investigation we have been able to discover more about the structure of the disk as it exists in the rod-shaped polymer by applying the three-dimensional reconstruction methods used previously to phase plate electron micrographs (Unwin, 1971), in which the contrast is more sensitive to changes in the projected density of the biological material, than it is to the negative stain. Such micrographs have been shown to display the azimuthal variations in specimen structure more effectively than the conventional bright field micrographs (Unwin, 1972).

The findings of the present three-dimensional analysis show some discrepancies with the earlier analysis from bright field micrographs by Finch & Klug (1971), which cannot readily be attributed to possible small variations in protein conformation between different particles. However, a further investigation (see accompanying paper, Unwin, 1974*b*) of bright field micrographs of the same specimens subjected to different electron doses indicates that these discrepancies can almost wholly be attributed to radiation induced effects involving a redistribution of the negative stain and to the above mentioned differences in the imaging methods.

2. Methods

In order to achieve the best possible results in terms of contrast and signal/noise ratio, the specimens were imaged in the electron microscope over very thin (<50 Å thick) carbon films, these being supported, in turn, on thick carbon films containing large numbers of holes. Negative staining was carried out in the usual way (e.g. Huxley & Zubay, 1960) using 1% uranyl formate solution.

Electron microscopy was performed with a Philips EM300 (C_S = 1·6 mm) operating at 100 kV. The method for taking phase plate images is described in detail elsewhere (Unwin, 1974*a*). It entailed a high electron optical magnification (120,000×), as the focussing is critical with this type of image, and also a reduction of the intensity of the unscattered electron beam of greater than 25% to ensure that the protein and not the stain made the greater contribution to the contrast.

Images of well-preserved specimens, suitable for subsequent processing, were selected from a large number by means of optical diffraction. Since the particles possess both cylindrical and helical symmetry, the optical diffraction patterns display two distinct

types of peaks: (a) those giving information on the cylindrically averaged radial and longitudinal variations in protein density (i.e. involving the J_0 Bessel function) and (b) those giving information on the azimuthal variations (which involve Bessel functions of the type J_{17}, J_{34}, etc.). The selection was governed by the intensity and sharpness of these peaks, and the degree of symmetry in their positions about the meridian.

Densitometry and Fourier transformation of areas boxed off to include one repeat distance (i.e. 10 disks), and their subsequent correlation and averaging were carried out by procedures developed in this Laboratory (see DeRosier & Moore, 1970, and L. A. Amos, manuscript in preparation).

3. Collection of Data

(a) *Preliminary steps*

A careful study of many images showed the stacked disk specimens to differ slightly, irrespective of their general state of preservation. The apparent widths of the holes down their centres, for instance, were not entirely constant (see also Finch & Klug, 1974). There was no evidence, however, that the variations were other than continuous, i.e. that there was more than one class of particle. We required a representative three-dimensional reconstruction, and therefore chose to compute an average structure using the average Fourier transform computed from a small number of the best preserved specimens, in which some such variation was evident, as the basis. Our intention was also to reconstruct the individual specimens. This would enable us to examine the three-dimensional source of the variation seen in projection and to obtain an assessment of the significance of our findings for the average reconstruction.

Five regions of specimen were selected for processing and these are identified in Plate I by rectangular boxes drawn over the photographs. Each region was converted into a two-dimensional array of some 12,000 density points by scanning the original plates with a microdensitometer having a step size corresponding to 3 Å. These arrays were then manipulated, following the methods of DeRosier & Moore (1970), to obtain Fourier transforms with phase origins positioned precisely on the particle axes (see Finch & Klug, 1971).

Having carried out these procedures for all five particles, a search was conducted (to a resolution of ~8 Å) for layer lines in their transforms, the positions of which were consistent with the helical selection rule (Finch & Klug, 1971,1974): $l = (3/17)n + 10m$ (where l is the layer line number, n is the order of the Bessel function involved and m can have any integral value), the amplitudes on which were higher than the local background level and the phases on which were consistent with those expected from a helical particle†. Typically, in this way, we were able to make tentative identifications of about 20 layer lines in each transform.

These layer lines were to be subjected to further analysis and were corrected at this stage for the amplitude attenuation due to the phase plate's interception of some of the scattered electrons in the microscope (Unwin, 1972). The imaging conditions were such that it was not required to compensate for the effect of the contrast transfer function on any layer lines other than the equator, this layer line being the only one involving very low spatial frequencies (see Fig. 2).

† The difference in phase between corresponding peaks on either side of the meridian are, ideally, 0° for n even and 180° for n odd (Klug *et al.*, 1958); we accepted deviations from the ideal figures of up to 50°.

(b) *Elimination of "spurious" peaks*

It is possible that in the above search a number of the layer lines were identified fortuitously: they may have originated, for example, from distortions or irregularities in the substrate or in the stain distribution rather than from structural features that were characteristic of the specimens. It was therefore considered essential to subject the data to a much more stringent test, such as demonstrating a reasonable consistency in structure factors from one particle to the next.

In order to carry out this test it was first necessary to determine the relative scales, axial shifts and rotations of each particle with respect to a given reference particle, and which way up each was in the densitometer array. Fortunately, all these parameters, with the exception of the relative rotations, can be determined from just those layer lines involving the J_0 Bessel function (i.e. those which are multiples of 10) where the peaks are generally stronger and hence more reliable. We therefore treated these data first, leaving the relative rotations to be determined from the remaining data at a later stage.

The procedure adopted was to take the transform of one of the particles (particle 2) as a reference, apply small axial shift and scale increments to each of the remaining transforms, calculate for these the revised and Friedel related structure factors, and then search for the conditions providing the minimum phase residuals, given by:

$$R(\delta z, \delta\phi) = \sqrt{\frac{\sum|\bar{F}|(\delta\theta)^2}{\sum|\bar{F}|}},$$

where $|\bar{F}|$ is the mean amplitude for corresponding points in the transform considered and in the reference transform, and $\delta\theta$ is their phase difference.

Having determined in this way the parameters giving the best fit of each particle with respect to the reference particle, it was possible to see by inspection if any layer lines were included that did not show reasonable interparticle correlation (we expect the phases of the main peaks to differ by no more than 50° from the average). No such layer line (to the 60th) was discovered, although peaks on the 30th and 50th layer lines of particles 1 and 2, which correlated between these particles, were absent in the remaining transforms.

By next applying small rotation increments to the remaining (azimuthal) data and again searching for minimum phase residuals, the complete orientation of each particle with respect to the reference particle was determined. This now made it possible to see if the azimuthal data were reproducible between particles.

A very thorough and careful examination of the structure factors along each of the appropriate layer lines in each transform in turn led to two main findings. One was that the layer line data from particle 3 were significantly poorer than the layer line data from the remaining four particles (suggesting that there is a relatively high degree of azimuthal disorder in this particle), and the other was that only about two-thirds of the layer lines tentatively identified previously could be correlated satisfactorily between all the transforms.

The azimuthal data from particle 3 and the layer lines which did not exhibit consistent interparticle correlation were accordingly omitted from the data which were to be processed further (see below). It is notable that of the layer lines remaining, all (except for the third; see Discussion section (c)) appear to have a fairly strong counterpart in the X-ray diffraction pattern from oriented sols of stacked disk rods (Finch & Klug, 1974).

(c) *Average structure factors*

The establishment of the relative orientations of the individual particles made it possible to calculate the average structure factors directly. We did this, still treating the "J_0" and the azimuthal data separately, by combining the data from both sides of each transform and thereby obtaining the average of 10 or 8 half layer lines. We then compared the two sets of averaged structure factors with the individual sets of data (average of two half layer lines). This comparison yielded the minimum phase residuals given in Table 1.

TABLE 1

Minimum phase residuals (in degrees) of individual transforms relative to the average

Particle	$R(\delta z)$	$R(\delta z)_{\text{u.d.}}$	$R(\delta\phi)$	$R(\delta\phi)_{\text{u.d.}}$
1	25	47	36	64
2	30	44	33	66
3	42	48	—	—
4	41	52	35	74
5	40	52	36	71

Referring to the J_0 data first, we observe that the residuals, $R(\delta z)$, are considerably lower for particles 1 and 2 than for the rest. This suggests rather better preservation of the longitudinal and radial variations of protein density in these two particles. A further point is that the differences between the residuals, $R(\delta z)$, and the corresponding upside down values, $R(\delta z)_{\text{u.d.}}$, are all of the same sign (negative). This would be consistent either with a polar packing of identical subunits in the two layers comprising the disk or with unspecified packing but dissimilar conformations of the subunits in the two layers.

The phase residuals, $R(\delta\phi)$, obtained from the azimuthal data and, as explained in section 3(b), pertaining to four transforms rather than to five, are of similar magnitudes to the $R(\delta z)$, indicating that the quality of the two sets of data is similar. Note also that in all cases $R(\delta\phi) - R(\delta\phi)_{\text{u.d.}}$ is negative, confirming that the polarities of the particles were previously determined correctly, and that the magnitudes $|R(\delta\phi) - R(\delta\phi)_{\text{u.d.}}|$ are large, substantiating the implications concerning the packing of the subunits drawn from the J_0 data.

In calculating the average structure factors for the azimuthal data we incorporated the scale factors and axial shifts deduced from the supposedly more reliable J_0 data. They were however also estimated from the azimuthal data alone. Such an independent estimate gave new values for the scale factors and axial shifts differing by not more than 0·5% and 0·75 Å from the original values. These discrepancies between the two types of estimate were considered sufficiently small to be neglected.

Figure 1 gives an idea of the variability in structure factors obtained for a typical strong layer line ($l = 7$) and a layer line on the acceptable limit ($l = 36$).

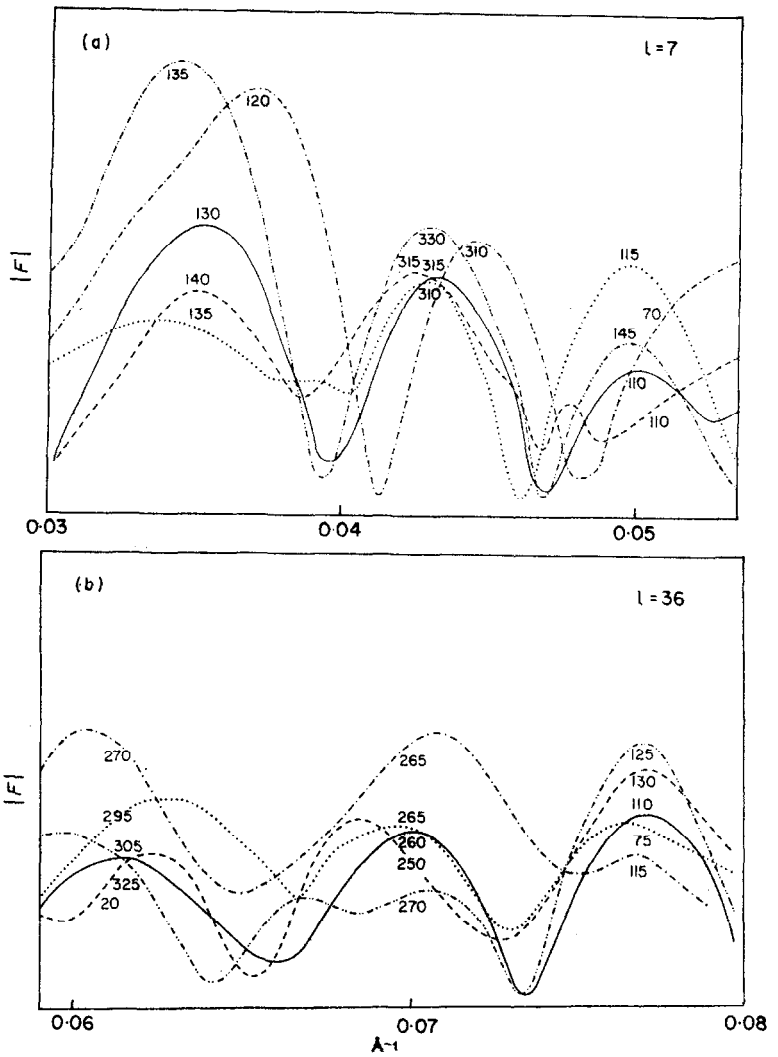

FIG. 1. Plots of the typical variations in amplitude, $|F|$, and phase angle found between particles for (a) a strong low resolution layer line (the 7th) and (b) a weak relatively high resolution layer line (the 36th). Each curve is the average of 2 sides and the phase origins for each particle are equivalent. (—··—··—) Particle 1; (· · · · ·) particle 2; (————————) particle 4; (—·—·—) particle 5; (————————) average.

(d) *Structure factor on the equator*

Since the negative stain wets both the specimen and the substrate, it is inevitable that its distribution round the specimens will not be cylindrically symmetric, even when the specimens are themselves undistorted. This means that reconstructions (which involve a Fourier–Bessel synthesis and hence assume cylindrical symmetry) incorporating equatorial structure factors from conventional images are unlikely to provide accurate representations of the radial density distributions. With equatorial structure factors from phase plate images, on the other hand, one might expect the

stronger contribution to the contrast from the (more cylindrically symmetric) biological material to make this problem less severe. Some evidence that this is indeed so is provided by the fact that we were able to derive radial density distributions from these images which gave sensible, near zero, densities in the region of the particle centres and at their outer extremities. Best results were obtained with particle 2 and the radial density distribution calculated for it is plotted in Figure 2.

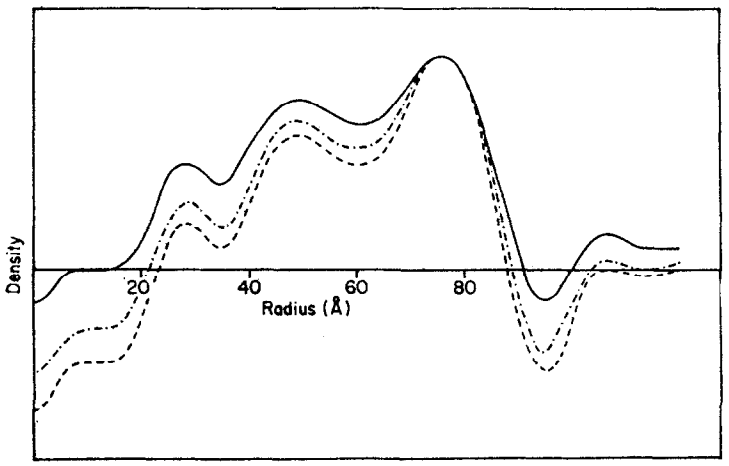

FIG. 2. Radial density distribution calculated from the structure factor on the equator for particle 2. (————) No corrections applied; (—·—·—) after correcting for the "absorption" of some of the scattered electrons by the phase plate in the microscope; (————) after correcting both for absorption and the effect of the contrast transfer function (see Unwin, 1972).

The two main minima on this curve, at radii of 35 and 60 Å, were consistent features of all equatorial syntheses. The other syntheses did not however give such satisfactory profiles in the region of the particle centres. A small degree of particle flattening could well be responsible for this and we therefore chose to incorporate the equator of particle 2, rather than an average equator, in the composite "average" Fourier transform, which is described below.

(e) *The "average" Fourier transform*

Figure 3 illustrates the form of the Fourier transform constructed from the structure factors averaged and calculated as in the two preceding sections. In this display the main diffraction peaks are represented as circles with areas proportional to amplitude and these are drawn over the line printer amplitude output for particle 2.

Comparing the two transforms we can note immediately that corresponding peaks match up quite well in position and amplitude, as of course should be expected. The relatively high background amplitudes shown by the transform of particle 2 (and similarly with the other transforms) would, in normal circumstances, cast doubt on the significance of the weaker peaks; however, we believe that their retention is justified on the grounds that their phase correlation across the meridian, as well as their reproducibility between particles in terms of absolute phase (Fig. 1), is good.

An encouraging feature of this average Fourier transform is its fairly close resemblance to the X-ray diffraction pattern from the oriented sols (Finch & Klug, 1974). The particular way in which the two patterns do differ is discussed in section 4.

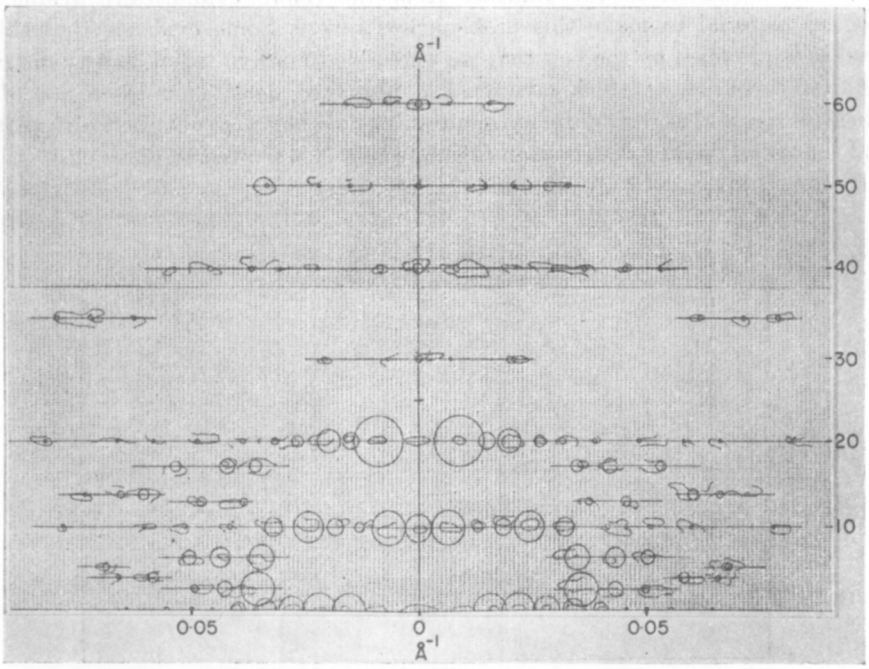

FIG. 3. The "average" Fourier transform drawn over the line printer amplitude output for particle 2. The amplitudes are proportional to the areas encircled and are indicated for all the major peaks except for the extremely intense meridional peak on the twentieth layer line and the two most intense peaks on the equator. The circles on the layer lines $l = 10m$ represent an average of all 5 particles, the equator is from particle 2 and the remaining layer lines are from particles 1, 2, 4 and 5.

4. Three-dimensional Reconstructions

(a) *Cylindrically averaged structure*

The cylindrically averaged structure is calculated by including only those layer lines which involve J_0 Bessel functions in the Fourier–Bessel synthesis, and a longitudinal section through it therefore provides a map which is independent of the effects of azimuth, but fully describes the cylindrically averaged radial and longitudinal variations in protein density (Klug *et al.*, 1958). Such maps were calculated for all five particles individually and also for the average, which is shown in Figure 4.

Particularly striking in this Figure are the differences in appearance between the two layers comprising the disk, the main body of the upper layer tending to follow a near radial line and the main body of the lower one tending to form a zigzag. The local bunching together of the layers within disks at the outside, but between disks on the inside, as found by Finch & Klug (1971), is also clearly evident.

The latter pairing phenomenon is well established, but its degree of variability from particle to particle, and also the nature of the departures of the two layers from 2-fold symmetry about a radial line drawn through the disk, are not. We accordingly studied these properties further. This involved a careful comparison of the individual maps and a statistical estimate of the random errors present.

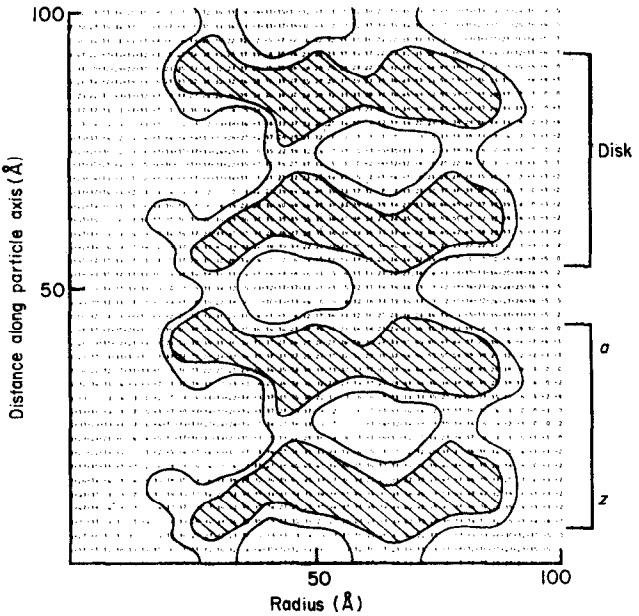

FIG. 4. Axial section through the cylindrically averaged structure; average of all 5 particles. For the notations *a* and *z* see text, section 4(b).

Errors in the Fourier–Bessel synthesis tend to accumulate along the particle axis, and the high positive densities existing in this region are therefore not structurally significant.

From the first study it was observed that for radii greater than ~50 Å the individual maps all showed the same basic patterns of density distribution (although obviously affected by noise) as indicated in Figure 4. On the other hand, for radii smaller than this there was quite a noticeable variation in the degree of bunching together of the layers of adjoining disks, closer bunching together (as with particles 1 and 2) having the effect of drawing the inner extremities of the layers away from the particle axis. This behaviour may account for the variations in the widths of the central holes observed in the micrographs. However, there was enough variation between reconstructions in the amount of matter in this region to suggest that differences in the state of preservation of the protein (resulting, for example, from proteolytic cleavage; Durham, 1972) could also be partly responsible.

To investigate the significance of the departures of the two layers from 2-fold symmetry we took each reconstruction in turn and subtracted the densities in the two layers dyadically (i.e. the densities in the array defining one layer minus the corresponding 2-fold related densities in the array defining the other layer). From the five resultant arrays thus produced, we obtained a best estimate of the standard deviation between reconstructions of 15·1 density units. This is equivalent to a standard deviation of $15{\cdot}1/\sqrt{5} = 6{\cdot}7$ for dyadic subtraction of the average reconstruction.

Now there were found to be two broad peaks in the latter subtraction, centred at radii of about 30 and 70 Å, which involved figures of at least twenty density units (~3 standard deviations). The departure of the two layers from 2-fold symmetry

in these two regions is therefore significant. From the positions of these peaks we can further conclude that the qualitative distinction made above between the two layers (i.e. one following closely a near radial line, but the other following a zigzag) is completely valid.

Other putative regions of departure from 2-fold symmetry, involving smaller density differences, have not been proved to be significant by this test. They should not be dismissed, however, since the estimates of the standard deviation would undoubtedly have been lower if account were able to be taken of genuine small variations between particles, such as are obviously evident at the smaller radii.

(b) *Full reconstructions*

The full three-dimensional reconstruction, computed from the entire data displayed in Figure 3, is presented as a model in Plate II. The density cut-off level for the model was chosen so as to just preserve continuity of the structure, this level being only 4% higher in the density range than the level one would predict in estimating the volume of protein by assuming it to have a molecular weight of 17,500 and an average density of $1{\cdot}27\times10^{-24}$ g/Å^3 (Mikhailov & Vainshtein, 1971).

From a sectional view of the model (Plate II(a)) we can identify the two large open spaces at radii of 45 and 70 Å which separate the layer following a near radial line from the layer forming a zigzag in the cylindrically averaged structure. The sectional view further shows the former layer (marked *a* in Plate II(a)) to have a set of angled holes running between the subunits at a radius of 55 to 60 Å, and the latter layer (marked *z* in Plate II(a)) to have a set of narrow grooves penetrating between the subunits from the outside in to a radius of about 60 Å. This latter groove is perhaps more obvious in the face-on view of the model (Plate II(b)) where it can also be compared with its shallow and broader equivalent in the other layer.

The subunits of the two layers of a disk come close together at a radius of about 80 Å, but whether they actually make contact here, as the model suggests, is doubtful since the regions involved are small in extent and involve densities which are very near to the cut-off density. The interdisk contact at a radius of 70 Å, and the intradisk contact at a radius of 45 Å, on the other hand, seem reasonably well established.

One gets very little indication of the paths followed by the subunits from the model, in which only one contour level is represented, but actual density displays in the form of cylindrical sections (i.e. two-dimensional arrays in which distance along the particle axis is the ordinate and the azimuthal angle is the abscissa) suggest that they can be traced fairly reliably as far in as to a radius of about 60 Å. Examples of such density displays are given in Figure 5. The pattern formed by their superposition in radial projection, which enables the course of the subunits to be visualized directly, is shown in Figure 6.

It is clear from Figure 6 that, in to a radius of 60 Å, the path taken by the subunits tends to be dominated by changes in *azimuth* in the layer which followed a near radial line in the cylindrically averaged structure, but by changes in axial dimension in the layer which formed the zigzag. Hence the notations *a* and *z* given to these layers in Plate II. It is also apparent from the changing angle made by the major axis of the elliptical cross-sections of the *a*-layer subunits that they are twisted or tilted with respect to those in the *z*-layer at the lower radii. These essentially low

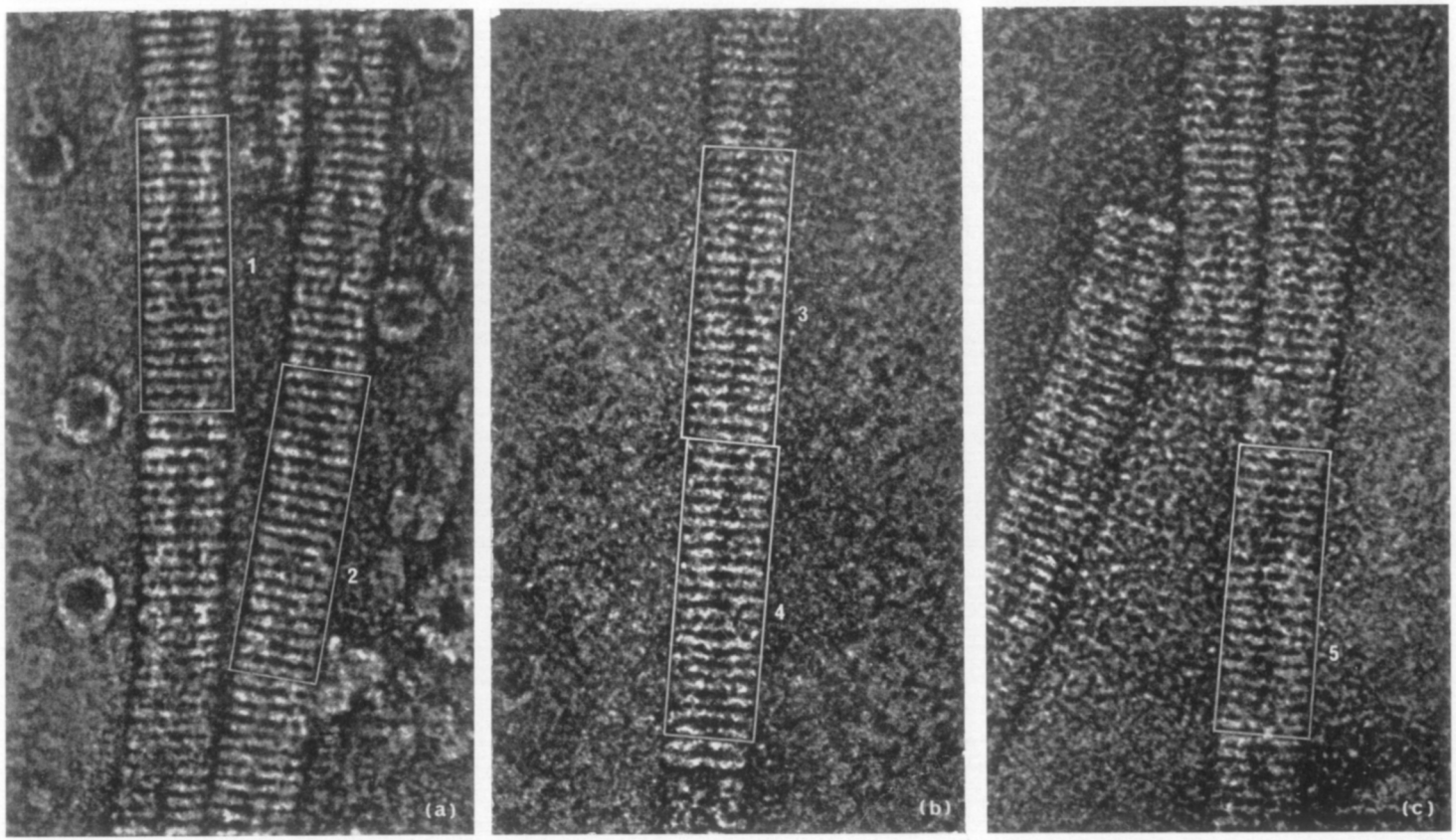

PLATE I. Phase plate images with the areas selected for processing (1–5) enclosed by rectangular boxes. The fraction of unscattered electrons allowed to contribute to these images was: (a) 0·5; (b) 0·7; (c) 0·7. In order to show a comparable range of grey levels in each case (a) was printed on less contrasty paper than were (b) and (c). Magnification 800,000×.

[facing p. 659

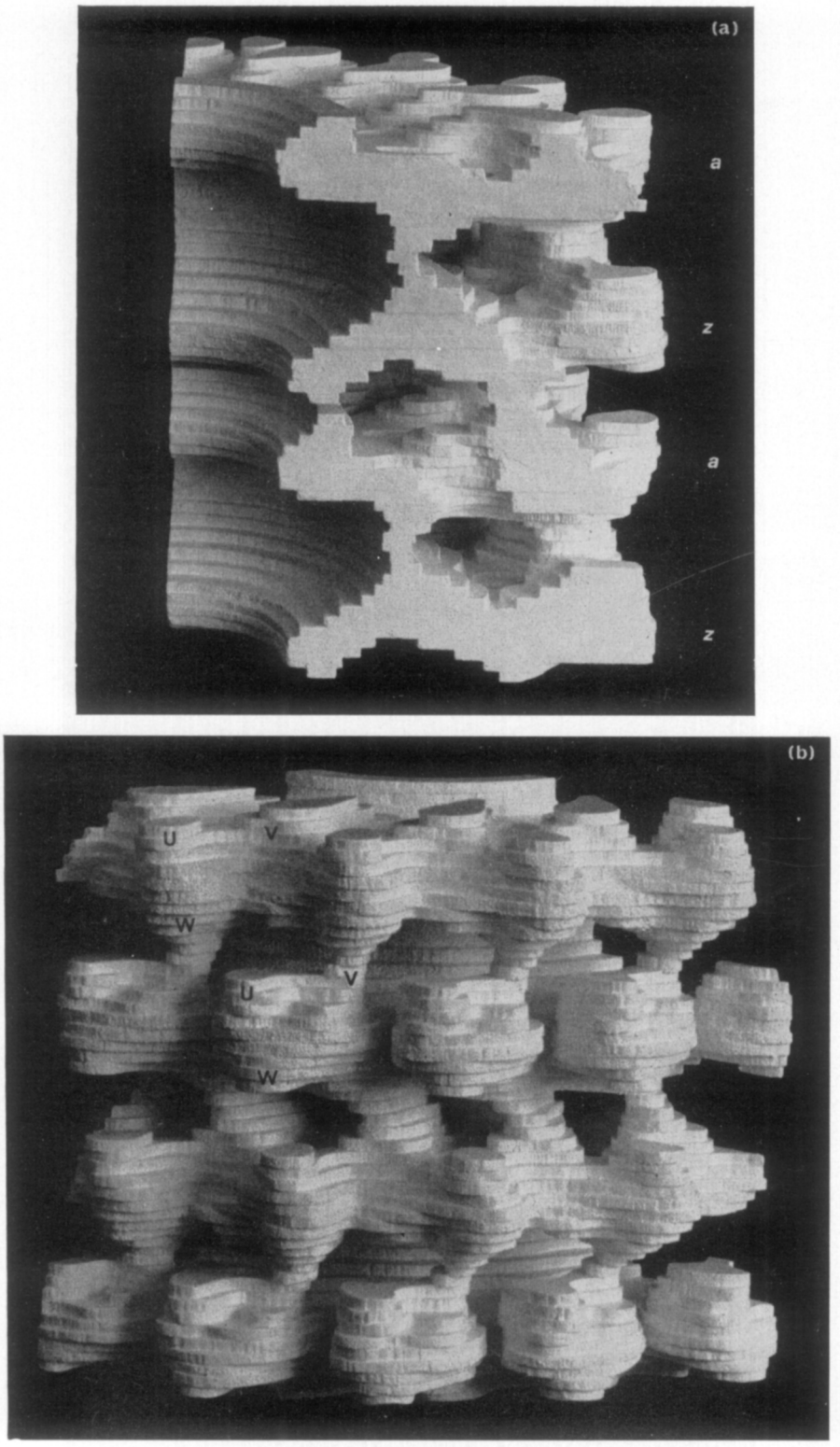

PLATE II. Two views of a model (90° section through two disks) of the stacked disk aggregate. (a) A sectional view (*a* and *z*-layers indicated) and (b) a face-on view showing predominantly the outer surface features. The letters in (b) mark points on the outer surfaces of the subunits which are adjacent to certain features identified on their faces; U and V refer to two "knobs" and W refers to a "ridge" (see text).

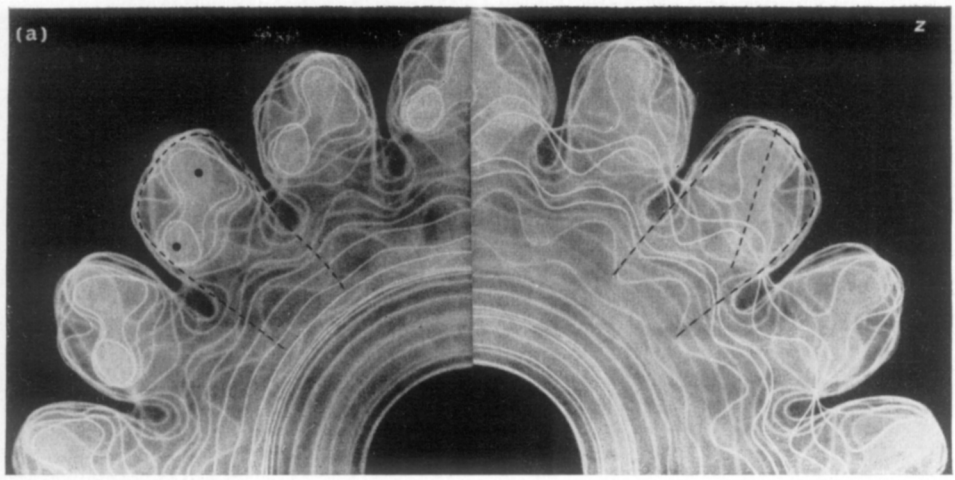

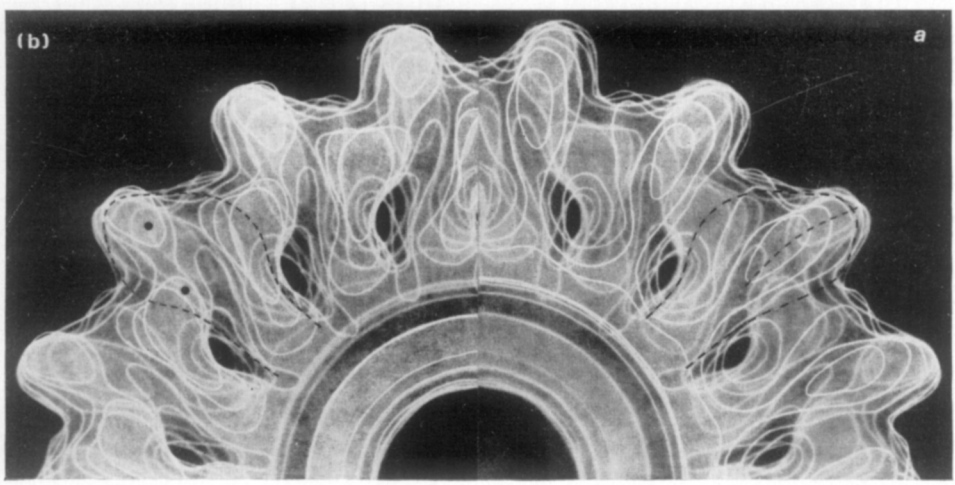

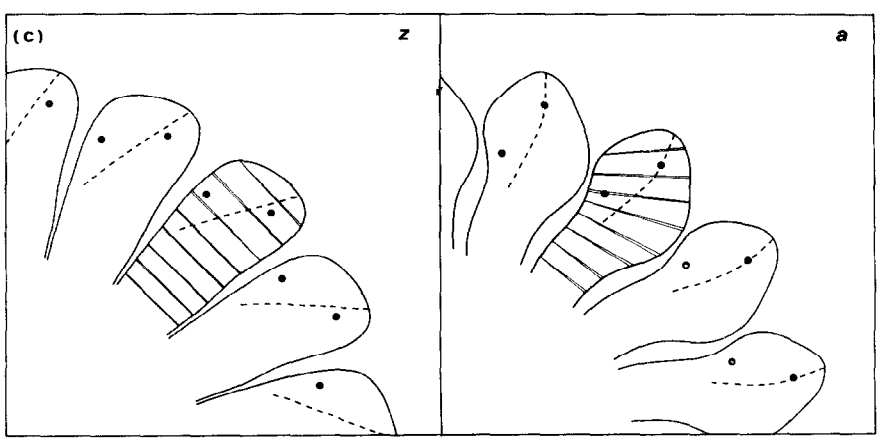

PLATE III. Contour maps (quadrants) viewed from (a) the upper and lower surfaces of the z-layer, and (b) the upper and lower surfaces of the a-layer. The sharpness of the contour lines gives a measure of their depth. The contour level is the same as the density cut-off level for the model. Markers drawn on the upper and lower surfaces of each layer, in order to identify features which appear to be common to both layers, are combined to form single projections in (c).

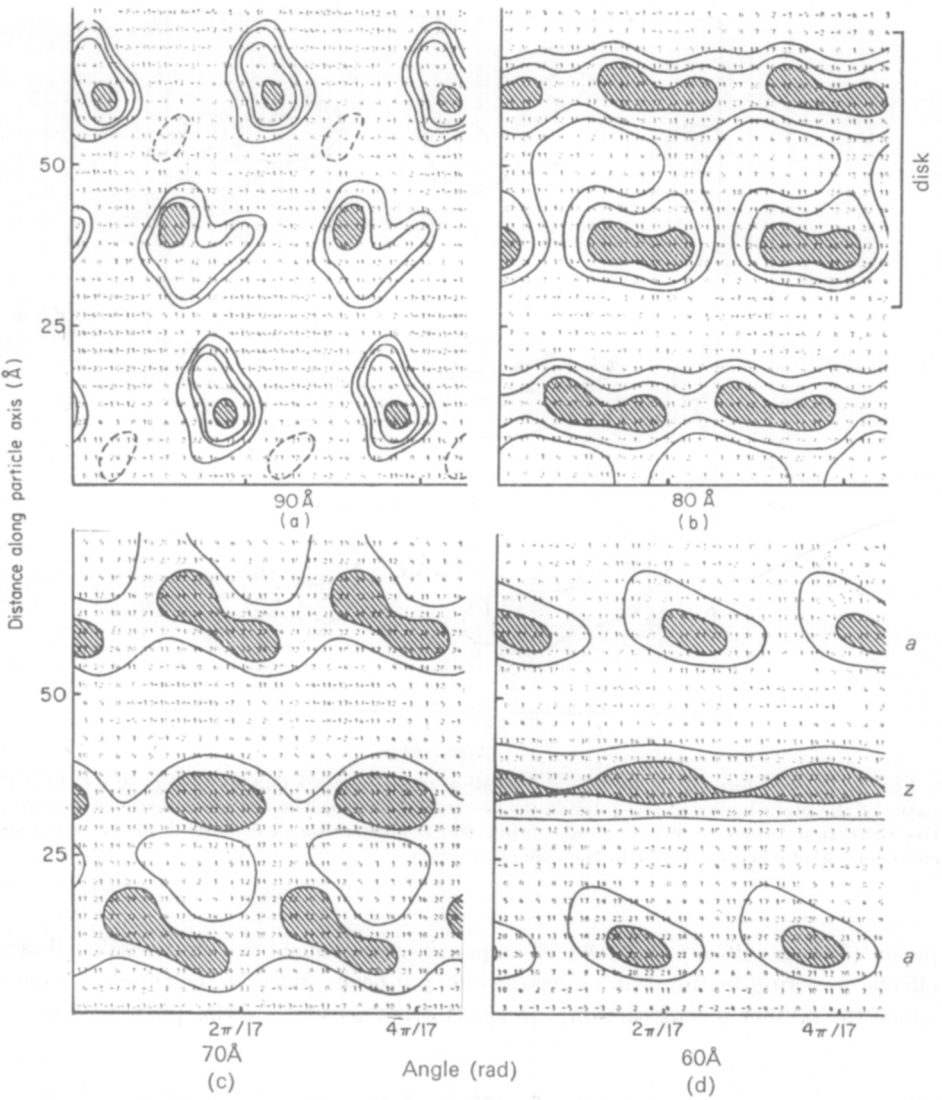

FIG. 5. Density distributions calculated from the average Fourier transform (Fig. 3) and displayed as cylindrical sections. Radii: (a) 90 Å, (b) 80 Å, (c) 70 Å and (d) 60 Å. The contours have been drawn at density unit levels of 15, 25, 35 and 45, and the regions enclosed by the highest contour levels in each case have been shaded.

The regions enclosed by the broken lines in (a) were found to be very sensitive to the relative weights of the third and seventh layer lines and to involve, at most, only low density figures in comparison with the regions enclosed by the full lines. They are therefore interpreted to be artifacts, not constituting a part of the real structure.

resolution differences in conformation between the subunits in the two layers are considered to be characteristic of the specimens since they were reproduced, at least qualitatively, in each of the individual reconstructions.

This description of the paths followed by the subunits is not entirely in agreement with the findings of Finch & Klug (1971), but it is demonstrated in the accompanying

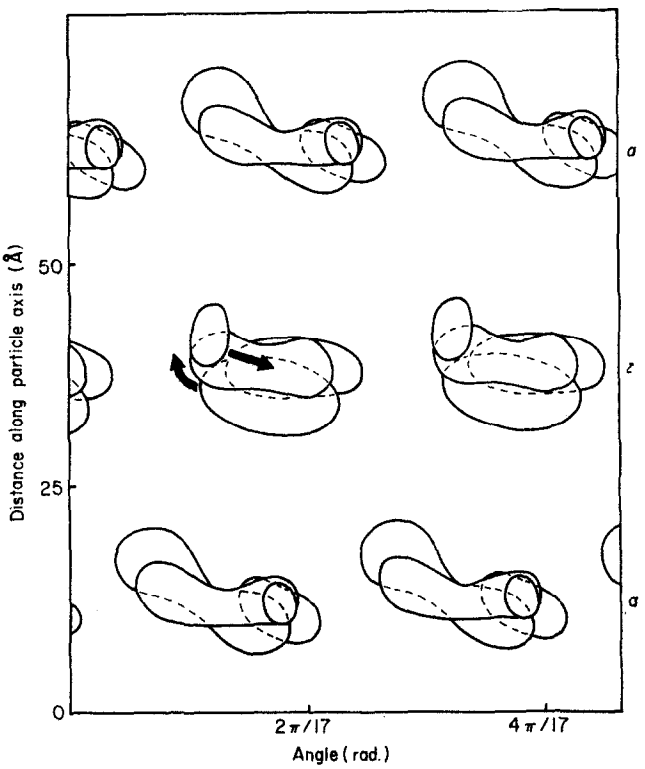

FIG. 6. Pattern formed by radial superposition of the shaded regions in Fig. 5, enabling the paths of the main bodies of the subunits to be easily followed. The arrows indicate the nature of the distortion proposed which would bring the conformation of a subunit in one layer into close correspondence with that in the other (see text).

paper (Unwin, 1974*b*) that the discrepancies concerned are due to redistribution effects occurring in the stain under the electron beam and that the type of image on which the present reconstructions are based is not sensitive to this phenomenon.

5. Discussion

(a) *Tentative correlation of features in the two layers of a disk*

An attempt was made to identify features which were common to each of the two layers comprising a disk, admitting the possibilities that they could be packed either dyadically or in a polar manner. Assuming that matter is distributed similarly along the lengths of the subunits, only the polar correlation produced a result which could in any way be described as satisfactory. Contour maps of each layer in the reconstruction from the averaged data are presented in Plate III to demonstrate this.

Referring first to the *z*-layer map (Plate III(a)), we identify the most obvious features on the upper surface of the subunits; that is the pair of "knobs" close to their outer extremities (dots in Plate III(a)) and their projected outlines (broken line in Plate III(a)). Next, we establish the positions of the equivalent features on the upper surface of the *a*-layer (Plate III(b)). Here there is only one readily identifiable equivalent feature—a knob. But there appears to be a good reason why the other

equivalent features are not immediately evident: the densities dividing the subunits in the *a*-layer are not sufficiently low in the region of radius of 70 to 80 Å for the contours (which are at the same level as chosen for the model) to be separated. It is in fact evident from the view in Figure 6, which shows the tilting and slewing of the subunits in this layer, where the projected outline and the equivalent of the second knob must lie. The positioning indicated in Plate III(b) is the only possibility. This new projected outline accounts for the apparently closer contact of the *a*-layer subunits at higher radii and their greater separation at lower radii (providing the obvious open spaces in the maps at 55 to 60 Å radius), as compared to the *z*-layer subunits.

Comparing next the two lower surfaces, the only prominent feature that can be readily recognized in both is a ridge, almost radial in the *a*-layer, but slewed quite strongly in the *z*-layer (it has only been outlined in to a radius of ~70 Å in Plate III, since the cylindrical sections indicate that its position in the *z*-layer would be unduly sensitive to small density errors at radii less than this).

That we are identifying the same ridge in each case relative to, say, the knobs on the upper surfaces, is corroborated by the geometry presented by these features at the outer surface of the model (Plate II(b)). It therefore is reasonable to combine these marks of identification into single projections, as in Plate III(c), to provide a picture of the way the two types of subunit seem to be related. The tentative nature of this correlation must, of course, be stressed: the identifications depend largely on high resolution detail and this is not fully reproducible between reconstructions.

(b) *Conformational relationship between the subunits in the two layers*

It was shown above how a tentative identification of certain prominent features on the subunits of the two layers of a disk could be made if it was assumed that they had the same polarity. We now attempt a simple reconciliation of their obviously different conformations by posing the question: can the marks of identification (Plate III(c)) on a subunit in one layer be mapped onto those on a subunit in the other without having to assume unlikely gross changes in the way matter is distributed within them?

To a first approximation, at least, it does seem possible to make this correlation. If, for instance, one were to rotate the "heads" of the *z*-layer subunits anticlockwise increasing amounts with increasing radius to imitate the slewing of the heads of the *a*-layer subunits, one might well expect the bend (of the zigzag) in the former at a radius of 70 Å to become less pronounced on one side (the tension side) than on the other, so that they become tilted (as in Fig. 6). This, on a simple mechanical scheme, would eliminate a large strain that would otherwise develop. Tilting, and hence a narrowing of the projection of the upper face of the *z*-layer subunits at lower radii to bring them into conformity with the projection displayed by the same face on the *a*-layer, is therefore certainly compatible with this movement (and *vice versa*). It is easy, moreover, to see that the rotating action is of such a nature as to make the two knobs and the ridge on the *z*-layer subunits match up closely with the equivalent features on the *a*-layer subunits, and hence make the outer regions of the subunits correspond.

Unfortunately, a more detailed interpretation than this of the relationship between the subunits is precluded by the tentative nature of the identifications made earlier,

the fact that the tilting and slewing of the subunits, while being qualitatively characteristic of all our reconstructions, are not reproducible in quantitative terms, and the fact that the negatively stained specimens do not give a completely realistic representation of the structure as it exists in solution (see below). It remains, therefore, only to emphasise the two most meaningful findings: (a) the qualitative agreement observed in the low resolution features of the individual reconstructions, and (b) the consistency of the overall appearance of the structure with these features when interpreted in terms of polar packing of conformationally related subunits. These findings together, we argue, provide strong evidence that the subunits in the two layers do indeed have the same polarity and are at least qualitatively related in the manner we have described.

(c) *Resemblance of the negatively stained specimens to their structure in solution*

The essential difference between the diffraction pattern derived above from the negatively stained specimens and the X-ray diffraction pattern obtained from sols of stacked disk rods can be seen by reference to the paper by Finch & Klug (1974). Using their terminology, it lies in the emphasis given to the "superlattice" layer lines (e.g. the third, tenth and seventeenth) relative to those which have equivalents in the X-ray diffraction pattern from helical polymers of TMV protein.

Since these superlattice layer lines can be considered to arise as a result of a "pairing" perturbation which is not evident in the X-ray pattern from the helical polymers (Finch & Klug, 1974), differences in their emphasis for the two cases must reflect differences in the magnitude of this perturbation, or the degree by which the two conformations of subunit within a disk differ. It is in the diffraction pattern computed from electron micrographs that these layer lines are stronger. Clearly then, the negatively stained specimens have somewhat exaggerated the conformational differences existing in the typical structure in solution.

Comparing the individual layer lines, we note that by far the most marked discrepancy between the computed and X-ray diffraction patterns occurs on the third layer line, the strong peak here in the computed diffraction pattern having only an extremely weak X-ray counterpart. This discrepancy is nevertheless not quite as serious as one might first suppose, since the position and width of the peak is such that it only gives information about the azimuthal distribution of matter over a very narrow region bordering the outer surface. Reconstructions made with the third layer line excluded from the synthesis suggest that the distortions from which it originates involve only minor displacements of material (of the order of 5 Å); such as could be simply accounted for in terms of a slightly diminished or exaggerated degree of slewing of the subunits in one or both of the layers.

Such distortions, it seems, could easily have developed during the final stages of drying of the stain or during the very early stages of irradiation.

Other discrepancies between the computed and X-ray diffraction patterns are too small to warrant detailed discussion. Indeed, taking account of the fact that only the general morphology of the protein is likely to be preserved in the negatively stained specimens (see Unwin, 1974), the agreement achieved is remarkably good. For example, the pattern of intensities discernible along the tenth and twentieth layer lines of the X-ray pattern can be followed quite closely in the computed diffraction pattern; the distinct closest-to-meridian peaks on the seventh, thirteenth and

seventeenth layer lines form the same patterns in either case; all the higher resolution peaks of the computed diffraction pattern can be identified with regions of relatively high intensity in the X-ray pattern.

The evidence therefore suggests that the present reconstructions, while slightly exaggerating the differences in the conformations of the subunits (especially in the region of their outer extremities), do otherwise provide a fairly faithful representation of the typical structure in solution.

(d) *Similarities between the stacked disk structure and other closely related structures*

The part of the present model which constitutes the *a*-layer has a number of features in common with the layer closest to the dyad axis in the structure recently determined by X-ray diffraction of crystals of disks (Gilbert & Klug, 1974). The obvious knob at the outer extremity and ring of density at the inner extremity of the *a*-layer are both characteristic of this layer in the X-ray structure; both structures show the subunits to be clearly separated at a radius of 55 to 60 Å, but less distinctly so at a radius of 70 to 80 Å; the path followed by the main body of the subunits both in the *a*-layer and in this "equivalent" layer of the X-ray structure varies axially only a small amount with increasing radius, not a relatively large amount as does the *z*-layer.

This resemblance between the *a*-layer and part of the crystal disk structure, together with the observed similarity (Gilbert & Klug, 1974) between the latter and the X-ray structure of the virus itself, suggests that the conformations of the protein molecules in the *a*-layer and in the virus are closely related.

Although the X-ray study of the disk in the crystal form did not allow the complete structure of the second layer to be determined, that part which was determined shows no evidence for the large axial variations clearly evident in the reconstructions of the *z*-layer. It therefore seems most likely that the subunits only have the particular conformation which is characteristic of the *z*-layer when they are assembled into stacked disk rods. This particular conformation may have arisen, in turn, as a result of the proteolytic cleavage known to have taken place in these polymers (Durham, 1972).

We thank Mrs L. A. Amos, Dr J. T. Finch and Dr P. F. C. Gilbert for helpful discussions.

REFERENCES

Butler, P. J. G. & Klug, A. (1971). *Nature New Biol.* **229**, 47–50.
Caspar, D. L. D. (1963). *Advan. Prot. Chem.* **18**, 37–121.
Crowther, R. A. & Amos, L. A. (1971). *J. Mol. Biol.* **60**, 123–130.
DeRosier, D. J. & Klug, A. (1968). *Nature (London)*, **217**, 130–134.
DeRosier, D. J. & Moore, P. B. (1970). *J. Mol. Biol.* **52**, 355–359.
Durham, A. C. H. (1972). *FEBS Letters*, **25**, 147–152.
Finch, J. T. & Klug, A. (1971). *Phil. Trans. Roy. Soc. (ser. B)*, **261**, 211–219.
Finch, J. T. & Klug, A. (1974). *J. Mol. Biol.* **87**, 633–640.
Finch, J. T., Leberman, R., Chang, Y. S. & Klug, A. (1966). *Nature (London)*, **212**, 349–350.
Franklin, R. E. & Commoner, B. (1955). *Nature (London)*, **175**, 1076–1077.
Gilbert, P. F. C. & Klug, A. (1974). *J. Mol. Biol.* **86**, 193–207.
Klug, A., Crick, F. H. C. & Wyckoff, H. W. (1958). *Acta Crystallogr.* **11**, 199–213.

Huxley, H. E. & Zubay, G. (1960). *J. Mol. Biol.* **2**, 10–18.
Mikhailov, A. M. & Vainshtein, B. K. (1971). *Sov. Phys. Crystallogr.* **16**, 428–432.
Unwin, P. N. T. (1971). *Phil. Trans. Roy. Soc. (ser. B)*, **261**, 95–104.
Unwin, P. N. T. (1972). *Proc. Roy. Soc. (ser. A)*, **329**, 327–359.
Unwin, P. N. T. (1974*a*). *Z. Naturforsch.* **29***a*, 158–163.
Unwin, P. N. T. (1974*b*). *J. Mol. Biol.* **87**, 657–670.